

Enhanced capacitive pressure sensing performance by charge generation from filler movement in thin and flexible PVDF-GNP composite films

Han Kim^a, Minseob Lim^a, Byungkwon Jang^a, Si-woo Park^a, Ji Young Park^b, Haishan Shen^b, Kangmo Koo^a, Hong-Baek Cho^a and Yong-Ho Choa^a

^aDepartment of Materials Science and Chemical Engineering, Hanyang University, Ansan, Republic of Korea;

^bInstitute of Environmental and Energy Technology, Hanyang University, Ansan, Republic of Korea

ABSTRACT

This study introduces an approach to overcome the limitations of conventional pressure sensors by developing a thin and lightweight composite film specifically tailored for flexible capacitive pressure sensors, with a particular emphasis on the medium and high pressure range. To accomplish this, we have engineered a composite film by combining polyvinylidene fluoride (PVDF) and graphite nanoplatelets (GNP) derived from expanded graphite (Ex-G). A uniform sized GNPs with an average lateral size of 2.55_{av} and an average thickness of 33.74_{av} with narrow size distribution was obtained with a gas-induced expansion of expandable graphite (EXP-G) combined with tip sonication in solvent. By this precisely controlled GNP within the composite film, a remarkable improvement in sensor sensitivity has been achieved, surpassing 4.18 MPa⁻¹ within the pressure range of 0.1 to 1.6 MPa. This enhancement can be attributed to the generation of electric charge from the movement of GNP in the polymer matrix. Additionally, stability testing has demonstrated the reliable operation of the composite film over 1000 cycles. Notably, the composite film exhibits exceptional continuous pressure sensing capabilities with a rapid response time of approximately 100 milliseconds. Experimental validation using a 3 × 3 sensor array has confirmed the accurate detection of specific contact points, thus highlighting the potential of the composite film in selective pressure sensing. These findings signify an advancement in the field of flexible capacitive pressure sensors that offer enhanced sensitivity, consistent operation, rapid response time, and the unique ability to selectively sense pressure.

ARTICLE HISTORY

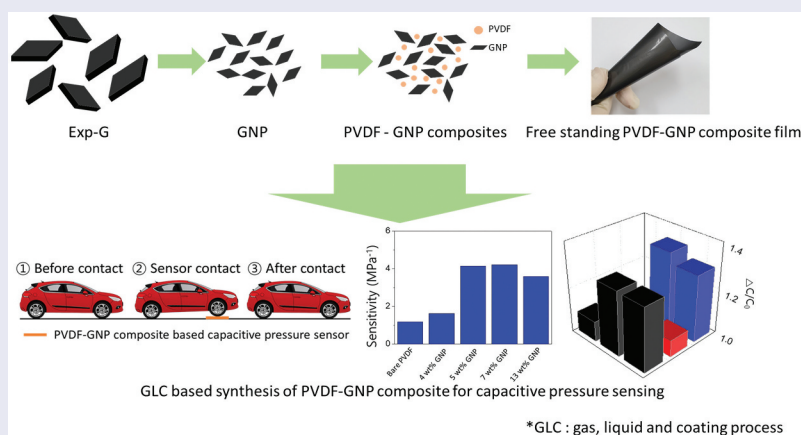
Received 29 June 2023

Revised 25 August 2023

Accepted 13 September 2023

KEYWORDS

PVDF-GNP composites;
capacitive pressure sensor;
dielectric layer; thin film





IMPACT STATEMENT


Our study provides the effect of GNP in a polymer composite system using a facile and easy process, to enhance the capacitive pressure sensing properties, particularly in high-pressure range applications.

1. Introduction

Sensing plays a crucial role in our daily lives as it helps alert us to potential accidents and maintain stability. Among the various factors that contribute to sensing,

pressure is particularly useful. Pressure derived from the contact force between two surfaces is useful to impose a sensing device because its signal change is intuitive, and it can convert electronic signals. As

CONTACT Yong-Ho Choa  choa15@hanyang.ac.kr  Department of Materials Science and Chemical Engineering, Hanyang University, 55 Hanyangdaehak-ro, Sangnok-gu, Ansan, Gyeonggi-do 15588, Republic of Korea

 Supplemental data for this article can be accessed online at <https://doi.org/10.1080/14686996.2023.2260301>.

© 2023 The Author(s). Published by National Institute for Materials Science in partnership with Taylor & Francis Group.

This is an Open Access article distributed under the terms of the Creative Commons Attribution-NonCommercial License (<http://creativecommons.org/licenses/by-nc/4.0/>), which permits unrestricted non-commercial use, distribution, and reproduction in any medium, provided the original work is properly cited. The terms on which this article has been published allow the posting of the Accepted Manuscript in a repository by the author(s) or with their consent.

a result, pressure sensors have become widely used in a range of industrial fields including robotics, aerospace, automobile, electronics, and biomedical, among others [1–3]. While conventional pressure sensors, which rely on mechanics, come in a wide range of pressures, from absolute to hundreds of MPa, they can be bulky and heavy, limiting their use in modern pressure sensing devices known as ‘microsensors’. Microsensors often require portability, flexibility, and lightweight design [2].

In response to these growing demanding factors, various flexible pressure sensors employing different transduction mechanisms such as piezoresistivity, capacitance, and piezoelectricity have been studied. Among these, capacitance-based pressure sensors have gained attention due to their advantages such as their simple structure, low power consumption, temperature independence, and mechanical robustness [1–3]. However, low sensitivity and limited pressure sensing range are seen as obstacles to their adoption in real-world devices.

In order to address this limitation, researchers have been focusing on the study of dielectric layer materials made of elastic polymeric materials, which are closely related to the performance of capacitive pressure sensors. There are various strategies for modifying the dielectric material, with the design of microstructures or porous structures being a commonly considered solution [4–10]. The elastic polymeric material such as polydimethylsiloxane (PDMS) is commonly used in this strategy. In the case of microstructures, designed mold or mask is used to fabricate the particular shape of a dielectric layer [4,7]. When considering the existing porous structure, the substances that can be readily eliminated through mechanisms like gas generation [5,9,10] or dissolution [6,8] is incorporated to dielectric layer. Although both microstructure and porous structure design can significantly improve sensing performance, they often require high cost and complex process for microstructure fabrication. Meanwhile, the design of a porous structure can lead to a mechanically weakened matrix owing to the presence of pores in the matrix and the pores on the surface of the dielectric layer can cause unstable connection with the electrodes. Consequently, the heightened sensitivity remains confined to low-pressure zones (1–10 kPa), and there continues to be reduced sensitivity in the medium (10–100 kPa) and high-pressure ranges (>100 kPa).

Given these considerations, polymer-filler composites are seen as an alternative strategy. The synergistic effect between the polymer and filler material allows for a low-cost, straightforward process while also providing improvement in mechanical and sensing properties [11–17]. Commonly, polymer-filler composites for this purpose consist of main polymer matrix and filler material. Polymeric materials such as PDMS,

thermoplastic polyurethane (TPU), and poly(vinylidene fluoride-trifluoroethylene) (PVDF-TrFE) are typically selected as a main matrix of composite because of their mechanical stability and elasticity [11,13,15]. Filler materials have mechanical stability and additional polarization for capacitive behavior when compression is induced, including silver nanowires (Ag NWs), carbon nanomaterials such as carbon black (CB), carbon nanotubes (CNTs) [11,12,14], and graphene [16,17].

Although these valuable efforts provide the strategy of extension of the pressure range or improvement of capacitive pressure sensing in medium and high pressure ranges, the range of pressure that shows stable sensitivity is still limited. Furthermore, the use of a dielectric layer with a large thickness, ranging from hundreds of micrometers to a few millimeters, could be a worrisome parameter to miniaturization of devices.

Herein, a thin and lightweight polyvinylidene fluoride (PVDF)–graphite nanoplate (GNP) composite film was investigated as a dielectric layer for a capacitive pressure sensor. The PVDF serves as the main polymer matrix for the dielectric layer, while the GNP was added to increase the sensitivity and response of the sensor. The composite paste was easily obtained through simple acoustic mixing, and the free-standing composite film was readily detached from an aluminum foil after being dried on a hot plate. The obtained composite film with a thickness of tens of micrometers was assessed as a potential option for the dielectric layer in a capacitive pressure sensor. The study also evaluated the composite film’s suitability for continuous and selective pressure sensing, while also anticipated how the concentration of filler in the composite affects the capacitive pressure sensing mechanism.

2. Experimental methods

2.1. Materials

Expandable graphite (Exp-G) was purchased from Sigma Aldrich (U.S.A.). N-Methyl-2-pyrrolidone (NMP) was supplied by Daejung chemicals and metals (Republic of Korea). PVDF was obtained from Arkema (France).

2.2. Fabrication of the PVDF-GNP composite film

The overall process of this research is illustrated in Figure 1. Exp-G was chosen as the starting material for GNP dispersion. To obtain expanded graphite (Ex-G), Exp-G was thermally treated at 900°C for 3 min. After as-prepared expanded Ex-G was carried into NMP, GNP dispersion was obtained by the tip sonication process using a tip probe sonicator (VCX-750,

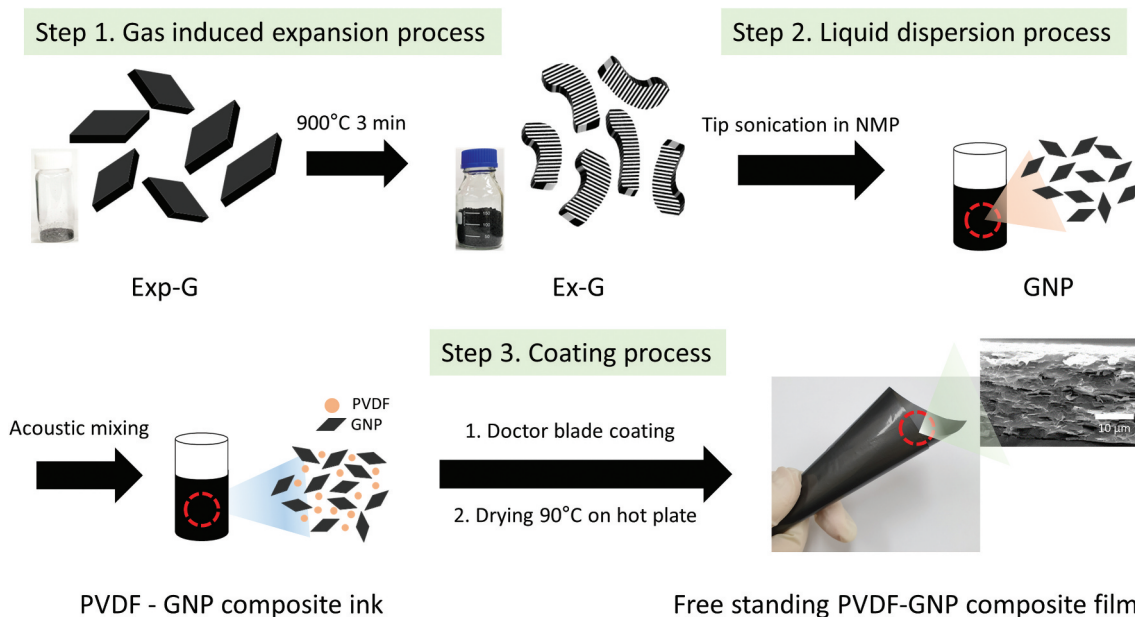


Figure 1. Overall experimental process of this research.

Sonics, U.S.A.). GNP dispersion was poured into a vial that contains PVDF, and then it takes place in acoustic mixer (pharma RAM1, Resodyn, Republic of Korea) to get PVDF-GNP composite paste. The total solid content was fixed at 8 wt% for composite paste. For example, for obtaining the 4 wt% GNP sample, the mass ratios of PVDF:GNP:NMP (as a solvent) are 7.68 0.32:92. The composite paste was coated on aluminum foil using a doctor blade with a settled wet thickness and dried on a hot plate at 90°C overnight. The fully dried PVDF-GNP composite film was easily detached from aluminum foil. The obtained free-standing film thickness was $35 \pm 3 \mu\text{m}$ for all the samples.

2.3. Characterization

The dispersibility change evaluation of GNP dispersion about real time was recorded using a Turbiscan instrument with the T-LOOP module (Turbiscan Lab, Formulation, France). The morphology of GNP was characterized using a field-emission scanning electron microscope (SEM; Mira3, TESCAN ORSAY HOLDING, a.s., Czech Republic) and a Transmission Electron Microscope (TEM; JEM-2100, JEOL Ltd., Japan). Lateral size and thickness distribution of GNP were analyzed using an atomic force microscope (AFM; XE-100, Park systems, Republic of Korea). The morphology of the PVDF-GNP composite film was also scanned by SEM. Electrical conductivity of the nanocomposite film was calculated from the sheet resistance measured using a 4-point probe auto contact system (CMT-SR1000N, AIT Co., Ltd., Republic of Korea), and film thickness was measured using a digital micrometer (IP65, Mitutoyo, Japan). Crystalline phase was characterized by X-ray diffraction analysis (XRD; D/

MAX-2500/PC, Rigaku corporation, Japan) and Fourier-transform infrared spectroscopy (FT-IR; Nicolet iS10, Thermo fisher scientific Inc, U.S.A.). Thickness changes of the sample film with induced pressure are measured and calculated using an automated nanoindentation measuring system (Fischerscope HM2000, Helmut Fischer GmbH, Germany).

2.4. Performance of the capacitive pressure sensor

Pressure sensing performance was calculated using a handmade pressure sensing measurement system (Figure S1). It consists of a LCR meter (IM3523, HIOKI, Japan), a digital multimeter (DMM6500, KEITHLEY, U.S.A.), an Arbitrary waveform generator (3390, KEITHLEY, U.S.A.), load cell (MNC-50 L, CAS, Republic of Korea), and a pressure sensing measurement program (LabView, National Instruments, U.S.A.). The sample for the pressure sensor is made of the sandwiched structure consisting of the PVDF-GNP composite film between Cu tape electrodes. To initiate the pressure sensing measurement process, the system captures the initial response of capacitance change over time at the measuring frequency of 100 kHz. Following a series of operational cycles to establish the stabilized response of the composite film, saturated raw responses are then gathered, amounting to a minimum of five cycles for each sample (Figure S2). These collected responses serve as the basis for sensitivity calculations across all samples. The each data point of the change in capacitance ($\Delta C/C_0$) was obtained from the average value of three samples for each concentration of GNP, with standard deviation. The feasibility test of the capacitive pressure sensor

was also evaluated using the same pressure sensing measurement system. For the test at continuous pressure, the PVDF-GNP composite film was set between the two of Cu the tape attached PET substrate and sandwiched by adhesion tape. Adhesion tape was attached except at the contact area between the composite film and Cu tape. Selective pressure sensing response was measured using the 3 cm x 3 cm array electrode which is the same structure as the capacitive pressure sensor device.

3. Results and discussion

3.1. Characteristic of PVDF-GNP composites

To achieve a uniform composite, finding the right solvent for the PVDF-GNP composite system was attempted. It is a known fact that graphite-based nanomaterials tend to aggregate due to their van Der Waals forces resulting from their conjugated atomic structure [18–21]. Hence, choosing the right solvent for GNP dispersion is crucial. Typically, when the solubility parameters, known as Hansen solubility parameters (HSP), of the solvent and material are similar, it is considered a feasible system for stable dispersion. Based on this, four solvents with diverse solubility parameters (indicated by blue circles in Figure 2(a)) were selected, and their time-dependent stability was analyzed through the same exfoliation process with tip sonication. The stability of the dispersion was measured using a turbiscan instrument, which operates on the principle of light scattering and transmittance. In the case of black-colored materials like GNP, the transmittance decreases when GNP is well dispersed in the solvent due to GNP’s scattering or absorption effect on light passing through the dispersion. Hence, an increase in transmittance indicates unstable GNP dispersion due to aggregation or

sedimentation of GNP. As depicted in Figure 2(b), DMF and NMP did not alter the transmittance of the dispersion, indicating that these two solvents are capable of maintaining stable GNP dispersion. Furthermore, DMF and NMP are known to be effective solvents for swelling or dissolving PVDF [23,24]. Between DMF and NMP, NMP was selected because the transmittance showed a plateau, unlike DMF that showed an increasing trend. Another reason why NMP is the best solvent among the four is its HSP distance [22]. The HSP distance is the distance between the solvent and solute Hansen parameters and is defined as R [22,25],

$$R = \sqrt{(\delta_{D,A} - \delta_{D,B})^2 + (\delta_{P,A} - \delta_{P,B})^2 + (\delta_{H,A} - \delta_{H,B})^2} \tag{1}$$

where δ_D is the energy from dispersion forces between molecules, δ_P is the energy from dipolar intermolecular force between molecules, δ_H is the energy from hydrogen bonds between molecules, A is the solute, and B is the solvent. In this equation, a smaller value of R indicates a higher compatibility between the solute and solvent. The HSP distance for the four solvents, calculated using the assumed Hansen parameter for nanosized graphite [25], were 35.33 for water, 9.52 for IPA, 6.51 for DMF, and 3.04 for NMP. This trend can also be applied to PVDF, with NMP being the best solvent for stable PVDF dispersion among the four, with a HSP distance of 2.16.

The as-prepared GNP has a lateral size of a few micrometers and a thickness of tens of nanometers, as shown in Figure 3(a). Graphite-based nanomaterials typically have a crystalline structure with hexagonal atomic ordering [26,27], and the selected-area electron diffraction (SAED) pattern in Figure 3(b) clearly indicates that the crystalline structures remain intact after the exfoliation step using tip sonication. The

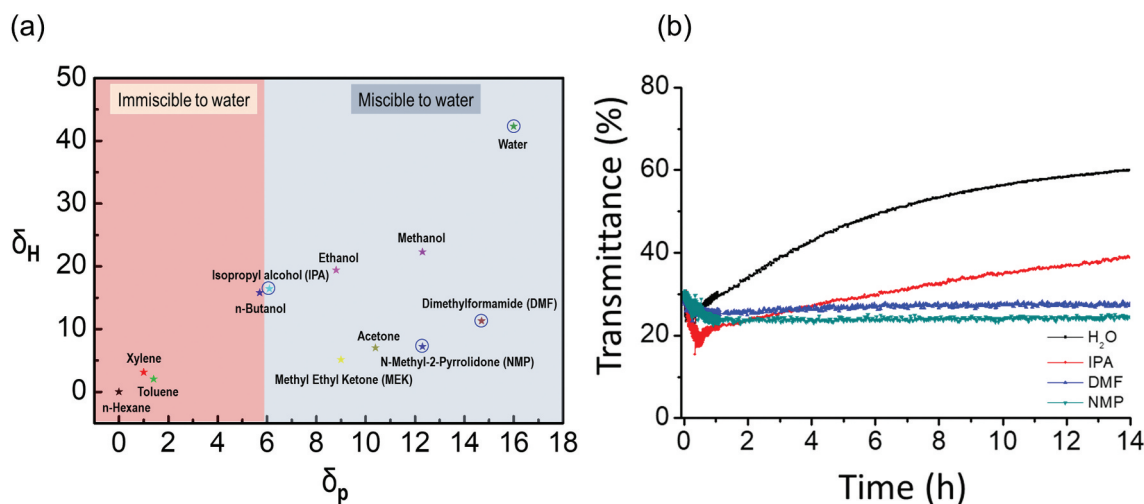


Figure 2. Dispersion stability data of GNP dispersion. (a) Solubility parameter of various solvents (δ_H : the energy from hydrogen bonds between molecules; δ_p : the energy from dipolar intermolecular force between molecules) [22] and (b) time-dependent dispersion stability change in various solvents.

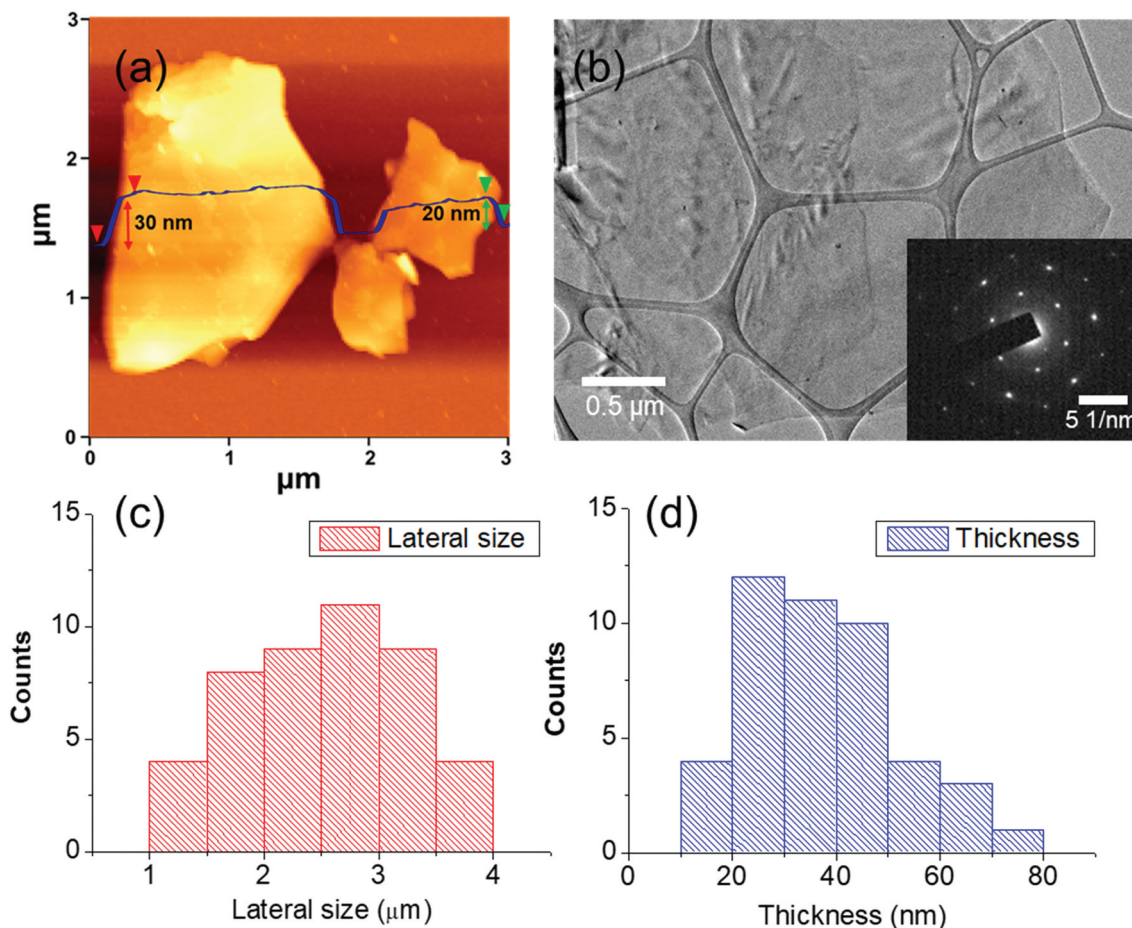


Figure 3. Morphology data of GNP. (a) AFM image, (b) TEM image (inset: SAED pattern), (c) average lateral size (red column), and (d) thickness (blue column).

morphological distribution of GNP is presented in Figure 3(c,d). Around 50 samples were collected to determine the average lateral size and thickness of the GNP. The results showed that the average lateral size of the GNP was $2.6 \pm 0.7 \mu\text{m}$, and the average thickness of GNP was $34 \pm 10 \text{ nm}$. Likewise, uniform results were consistently obtained across diverse batches, affirming the reliable structural integrity of GNP for the composite film fabrication. Additionally, a total of 50 samples per batch were also gathered to compare the average lateral size and thickness of the GNP (Figure S3).

The morphological distribution of the filler in the polymer matrix was characterized using SEM. As depicted in Figure 4, the morphology trend of GNP in the polymer matrix was exhibited. In the crumpled PVDF polymer matrix structure (Figure 4(a1–a3)), the density of the GNP particle which is well dispersed was increased (Figure S4), until the 7 wt% GNP concentration (Figure 4(b1–b3)). However, at higher GNP concentrations, such as 13 weight percent, the GNP particles displayed a stacked structure (Figure 4(c1–c3)). The results emphasize that even though the colloidal system typically prevents particle aggregation [28], it may not exhibit this beneficial effect for the entire range of filler concentration. In terms of the polymer-filler composite system, filler agglomerate

could be a major obstacle of deteriorating device performance. These results suggest that there is an optimal concentration point that can yield the best capacitive pressure sensing performance. Moreover, a uniform morphological outcome and consistent film thickness were observed across different batches of the composite film. This observation represents that the film fabrication process effectively guarantees the structural reliability of the composite film (Figure S5).

3.2. Capacitive sensing properties of the PVDF-GNP composite film layer

Capacitive pressure sensing performance could be evaluated from the change in capacitance value. The capacitance value of the PVDF-GNP composite film layer was measured using pressure sensing measurement system. Generally, Capacitance (C) could be expressed from the simple capacitor which consists of two parallel electrodes with a dielectric layer [1–3]

$$C = \frac{\epsilon A}{d} \tag{2}$$

where ϵ is the dielectric constant of the dielectric layer, A is the area between electrodes, and d is the distance between electrodes.

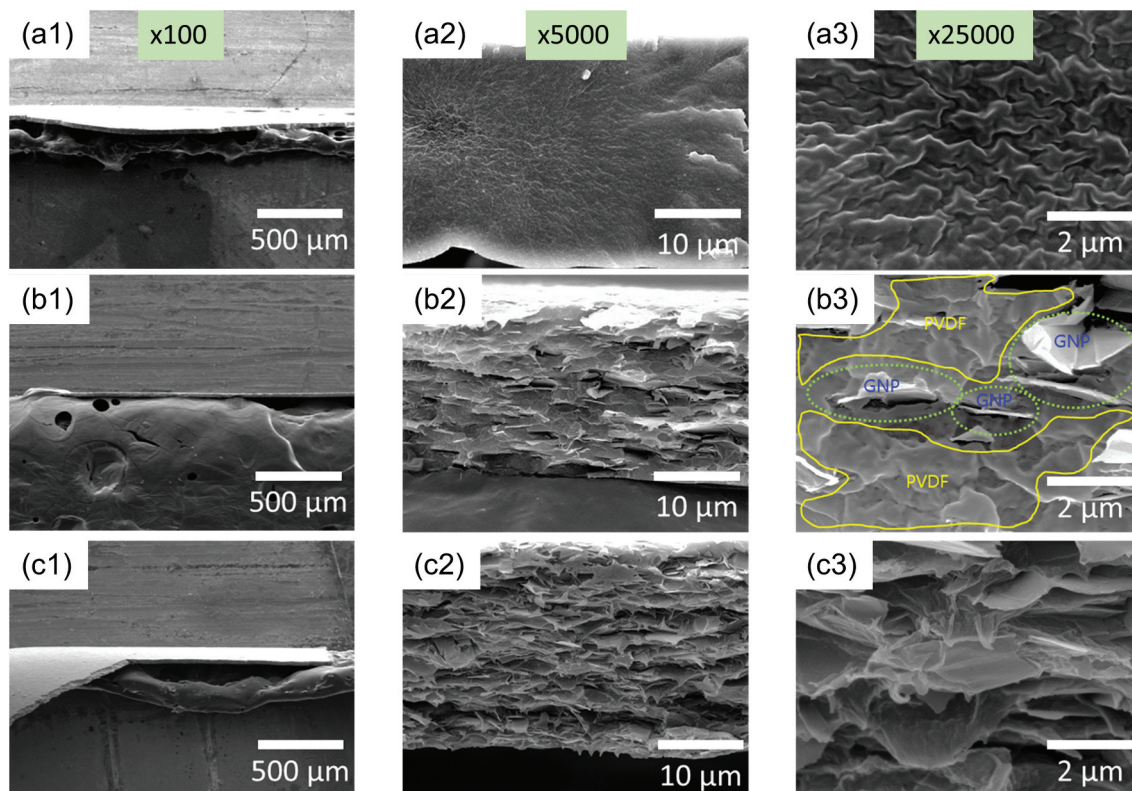


Figure 4. SEM images of the PVDF-GNP composite film. (a1–a3) bare PVDF, (b1–b3) 7 wt% GNP, and (c1–c3) 13 wt% GNP samples.

From the capacitance, sensitivity (S) of the capacitive pressure sensor could be calculated [1–3],

$$S = \frac{\frac{\Delta C}{C_0}}{\Delta P} = \frac{\frac{C - C_0}{C_0}}{P - P_0} \quad (3)$$

where P_0 is the base pressure and P is the pressure which is settled, C_0 is the base capacitance, and C is the capacitance after forced at pressure P .

The change in capacitance ($\Delta C/C_0$) is a crucial factor for determining the sensitivity of the sensor within the same pressure region. As demonstrated in Figure 5(a), the magnitude of $\Delta C/C_0$ increased upon the increasing GNP content up to 7 wt% under high-pressure conditions. However, this trend was not constant for all GNP content levels, as $\Delta C/C_0$ decreased at 13 wt%. This variation was also reflected in the sensitivity results, with the calculated sensitivity of 4.18 MPa^{-1} at 7 wt% and 3.58 MPa^{-1} at 13 wt% with acceptable linearity (Figure 5(b) and Table S1). These results indicate that there is a specific range of GNP content in the composite material that is optimal for its function, and this pattern was observed in the medium pressure range as well (Figure S6). The reason of this trend could be related to the electrical conductivity change of the composite. In the PVDF and GNP complex, GNP could exhibit the electrical pathway via the tunneling effect of electron, it causes increasing electrical conductivity until it reaches the optimum point named the percolation threshold [29,30]. Besides, after going through the percolation threshold, electrical conductivity value

arrives at a saturation point, showing that the exponentially increasing trend is typically limited and that the saturation point of performance is exhibited. The specific mechanism of this trend will be discussed in the next section. The PVDF-GNP composite film showed developed sensitivity and thin film thickness (Table S2). The cyclic stability was demonstrated using 7 wt% GNP sample to elucidate repeatability of the composite film. response of capacitive pressure sensing exhibits moderate stable capacitance changes after 1000 cycles applied pressure (Figure 5(c)).

3.3. Mechanism of capacitive pressure sensing of the PVDF/GNP composite film

From a capacitive perspective, the capacitance of a sensor is primarily influenced by the distance between the parallel electrodes, the surface area, and the dielectric constant. When compressive stress is applied, all these factors change, leading to a change in capacitance. The alteration in electrical conductivity observed under the application of compressive stress to the dielectric layer suggests the potential occurrence of several contributing factors. These factors might encompass variations in composite thickness, reconfiguration of fillers, and potential changes in the composite structure (Figure S7). Hence, it becomes essential to contemplate the primary factors influencing the capacitive pressure sensing performance within this intricate multicomponent system.

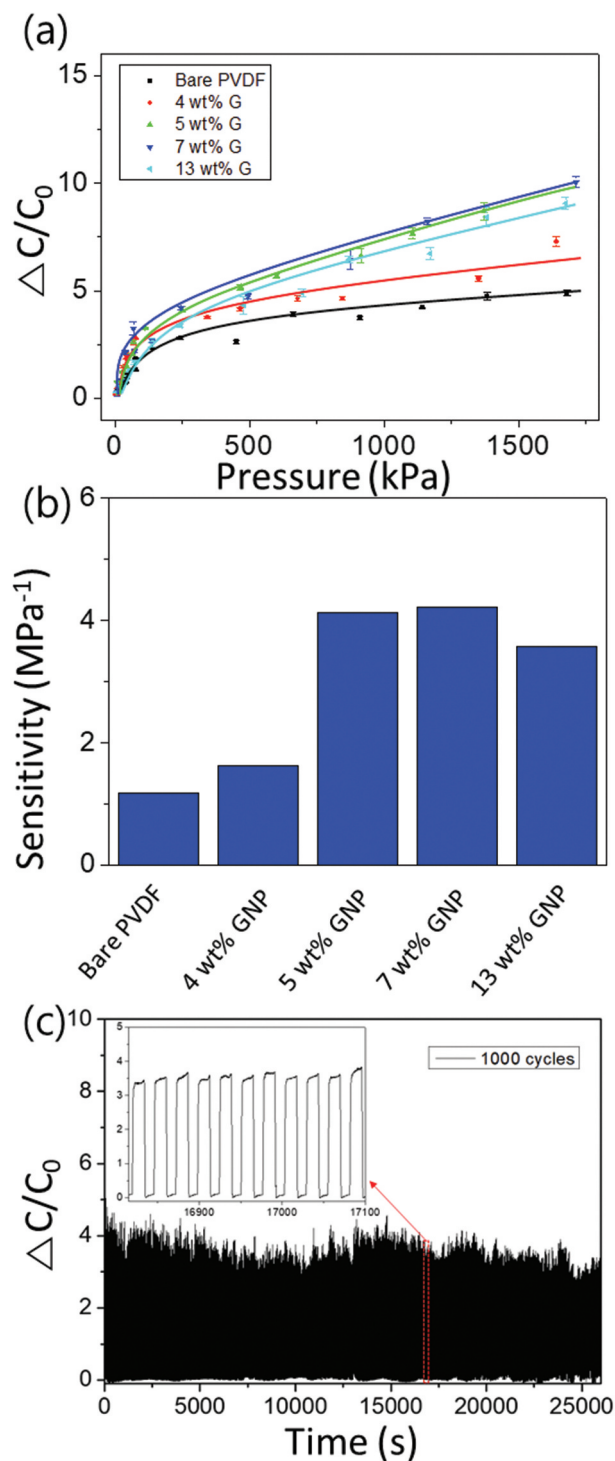


Figure 5. Capacitive pressure sensing performance of the PVDF-GNP composite film. (a) $\Delta C/C_0$ for pressure change and (b) sensitivity at 0.1–1.6 MPa (specific values are shown in Table S1) and (c) cycle stability of the PVDF-GNP composite film (inset: specific region data of sensing, the sample for cycle stability is 7 wt% GNP at 100 kPa).

The primary consideration is connected to the alterations in the composite film’s thickness, directly influencing the separation distance between the electrodes. If the dielectric layer exhibits flexibility, it can readily undergo substantial deformation and recovery, thereby significantly impacting the capacitive pressure sensing performance. To understand the extent of deformability within

this multi-component system across the range of 0.1–1.6 MPa, we conducted nano-indentation analysis to gauge the depth profile’s response to compressive forces, thereby quantifying the induced deformation strain. By correlating the applied pressure with the resultant change in thickness, we calculated deformation strain ratios of 0.48%, 0.50%, 0.49%, 0.60%, and 0.98% for the bare PVDF, 4 wt% G, 5 wt% G, 7 wt% G, and 13 wt% G samples, respectively. While this trend appears to positively influence the augmentation of capacitive pressure sensing performance, its impact may be less pronounced. Interestingly, the maximum sensitivity was obtained from the 7 wt% G sample, rather than the 13 wt% G sample, which exhibited the most substantial change in thickness. This observation suggests that factors beyond thickness alteration contribute to the sensor’s sensitivity.

The secondary consideration revolves around the influence of the crystalline phase in PVDF. Recognized as a piezoelectric material with a high piezoelectric constant, PVDF could significantly impact the polarization charge magnitude. Depending on its specific application, PVDF can exhibit three distinct molecular conformations (TGTG’, TTT, and TTTGTTG’) and manifest in five polymorphs, namely, phase 1 (beta (β)), phase 2 (alpha (α)), phase 3 (gamma (γ)), and δ , and ϵ phase. Of these, the β phase of PVDF is closely associated with the polarization charge magnitude due to its all-trans zig-zag conformation (TTT) [31,32]. This β phase can be induced through physical stress mechanisms such as stretching, quenching, straining, or polarization under a high electric field.

Given this relationship, the addition of GNP has the potential to induce alterations in the molecular structure or polymorph of PVDF, consequently having an impact on capacitive pressure sensing performance. To explore this phenomenon, all samples were subjected to characterization via FT-IR spectroscopy and X-ray diffraction (XRD) analysis to discern potential phase changes within PVDF. The results, as depicted in the obtained data (Figure S8), reveal no dramatic peak shifts across all samples. This suggests the absence of molecular structural changes attributed to the incorporation of GNP as an additional charge-generating filler. Considering these findings, it is speculated that the primary factor contributing to the enhancement of capacitive pressure sensing performance lies in the movement of the filler within the composite system.

When the compression is induced to the polymer composite, the movement of filler could lead to the increase in the vertical percolation threshold, that is, the disconnection between filler could be served [33]. This phenomenon could lead to increasing the disconnected filler density under the compression; in other words, the amount of filler, which can be polarize, is increased [11].

Taking into consideration the aforementioned background, a proposed mechanism for the effect of filler

alignment on capacitive pressure sensing is depicted in Figure 6. The alignment change of the filler can be divided into three parts with a similar trend in terms of the percolation threshold behavior of the polymer-conductive filler composite system (Figure S9). In case 1, there is not enough filler to form a conductive pathway, meaning that the distance between the fillers is too far to allow current to flow through the composite. Under these conditions, the alignment of the filler has little impact on the change in composite capacitance and results in a sensitivity similar to that of bare PVDF. In case 2, moderate connection between the fillers can be affected by the application of compressive force, leading to the deformation of the conductive pathway. This causes the non-connected fillers to function as an additional polarized part of the composite, resulting in an extra improvement in the change in capacitance. Notably, the findings of this study indicate that the region classified as case 2 exhibits the highest capacitive pressure sensing property in the composite material. This means that despite the fact that the concentration range of conductive filler is conventionally limited below the percolation threshold due to the presence of existing conductive pathways that reduce the polarized filler density, additional performance improvement could achieve at or above the percolation threshold in the composite system. This is attributed to the realignment of filler in the matrix that occurs upon the application of compression. Therefore, it could be possible to achieve a maximum performance point for the composite system at or above the percolation threshold.

Conversely, in case 3 of the composite film, where a high filler content is embedded, the conductive pathway is increased due to the reduction in the distance between fillers under compressive stress. Consequently, the change in capacitance diminishes within this region.

3.4. Consideration of the PVDF/GNP composite film as a component for the capacitive pressure sensing device

In terms of device application, PVDF has garnered significant attention as an appealing contender for self-powered devices, encompassing piezoelectric-based sensors, and nanogenerators, due to its elevated piezoelectric constant [34–36]. Despite the merits of piezoelectric-based devices, including self-power generation, favorable linearity, and a robust signal-to-noise ratio, certain limitations arise from their operating principles and conditions and the piezoelectric configuration necessitates a consistent force oscillation, as the accumulated charge disperses when the device reaches a static equilibrium. This phenomenon introduces considerable inaccuracies in static pressure measurements. Additionally, the operational window for viable pressure assessments remains constrained to higher ranges [37], effectively restricting the utility of piezoelectric-based sensors to specific environmental contexts. Moreover, achieving a substantial piezoelectric property is typically contingent on a significant presence of the β phase within PVDF. The induction of this β phase needs diverse extra physical stress

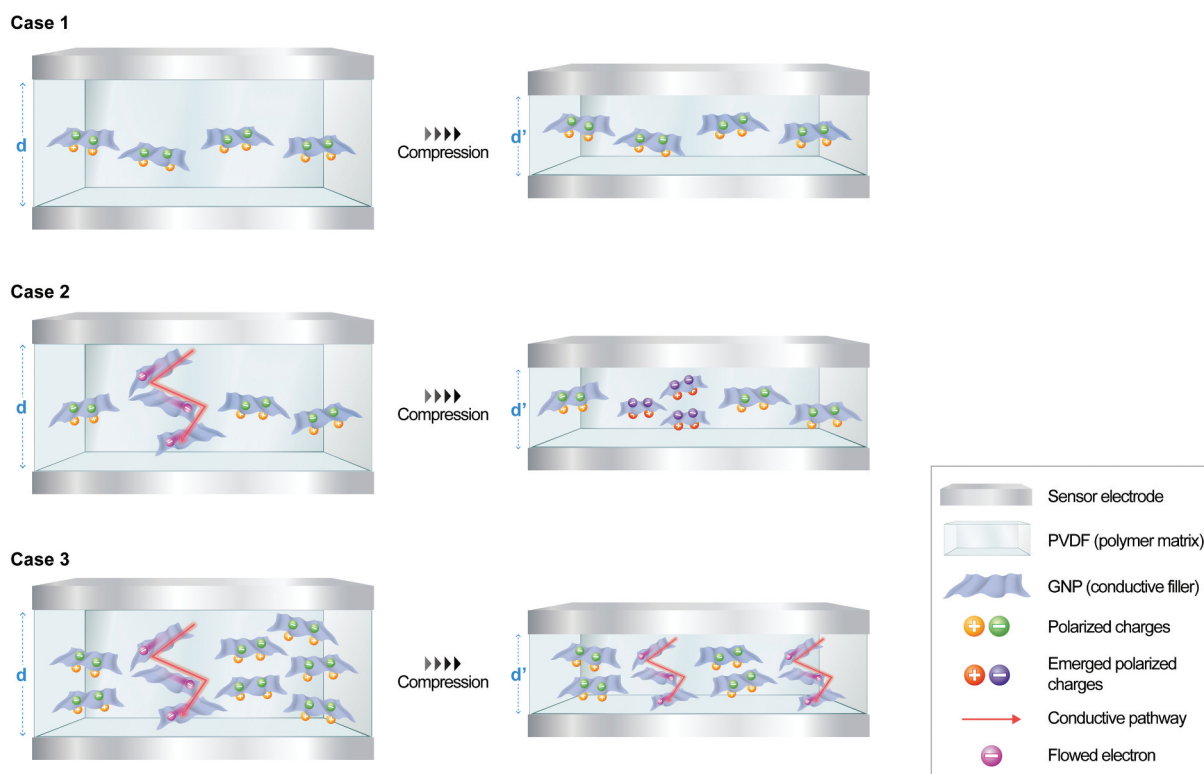


Figure 6. Expected mechanism of capacitive pressure sensing of the PVDF-GNP composite film (case 1: ≤ 4 wt%, case 2: $4 < x \leq 7$ wt%, and case 3: > 7 wt%).

mechanisms, such as stretching, quenching, straining, or applying polarization under a high electric field. Conversely, capacitive-based pressure sensors surpass these limitations, showcasing adaptability across a wide array of operational environments. This inherent advantage served as the bedrock of our research endeavor, compelling us to concentrate our endeavors on the progression of capacitive-based pressure sensing devices.

3.5. Demonstration of the capacitive pressure sensor

A simple capacitive pressure sensing device was demonstrated to detect continuous pressure changes under ambient conditions (Figure 7(a)). As shown in Figure 7(b), the device consists of a single layer of a PVDF-GNP composite film sandwiched between two copper electrodes. The device was attached to the ground, and a model car was moved in a backwards direction, which wound up a spring. The sensing response was recorded immediately upon contact between the model car and the device (this can be seen in Supporting Movie S1). The recorded response of the capacitive pressure sensing is shown in Figure 7(c). When the model car ran over the sensing spots on the

device, two types of responses were obtained; one from the front wheel and the other from the rear wheel. It was confirmed that the rear part of the car is heavier than the front part because the spring is attached at the rear, which results in a trend of the second response being larger than the first. This trend becomes even more pronounced as the weight of the model car increases, resulting in a larger C/C_0 value.

To assess the speed at which the device can detect pressure changes, the response time (T_{90}) and recovery time (D_{10}) were measured and are shown in Figure 8. Capacitive pressure sensing response was recorded well even when the sample weight was changed (Figure 8(a-c)), the response time was about 100 milliseconds (specific values of T_{90} and D_{10} are shown in Table S2) regardless of the weight of samples (Figure 8(d)), and the results are the same at the recovery step of capacitive pressure sensing (Figure 8(e)). These results insist that the time of sensing response is stable in the available pressure sensing range.

Lastly, we fabricated the capacitive pressure sensing array with the scale of 3×3 pixels to prove feasibility in selective area pressure (Figure 9(a)). As the selective area of pressure was induced (Figure 9(b)), the pixel point which was in contact between the sample and the array (Figure 9(c))

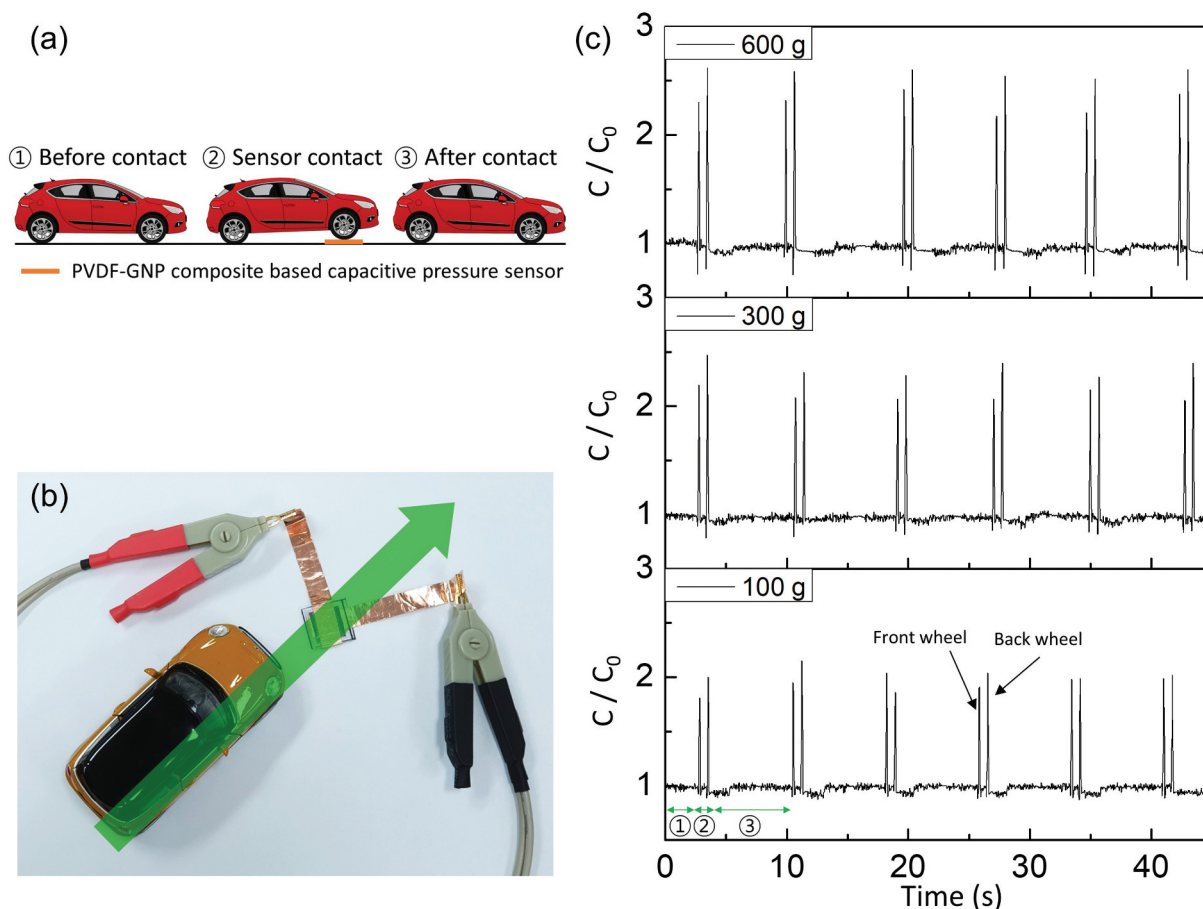


Figure 7. Demonstration of the simple capacitive pressure sensor at continuous pressure. (a) Operation steps, (b) snapshots of the configuration of the capacitive pressure sensing measurement, and (c) the C/C_0 response of the capacitive pressure sensor (7 wt% GNP sample was used as a dielectric layer of the sensor).

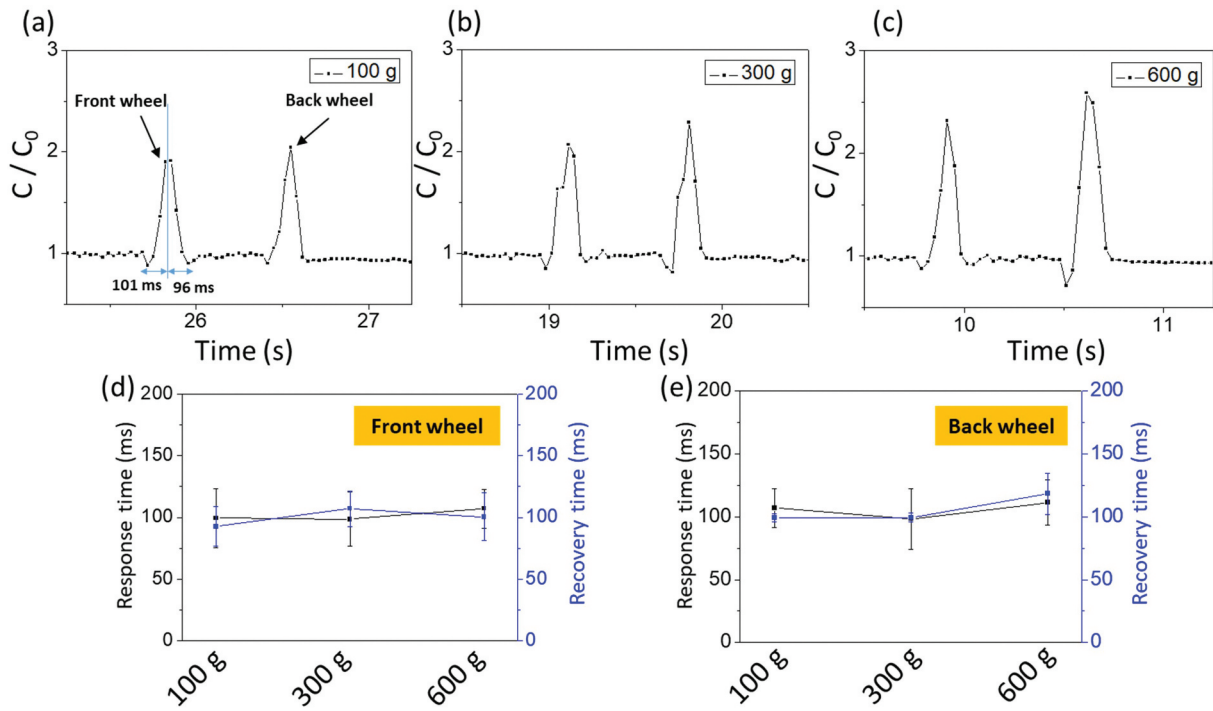


Figure 8. Capacitive sensing response of (a) 100 g, (b) 300 g, and (c) 600 g sample, response and recovery time of (d) front wheel and (e) back wheel of the capacitive pressure sensing sample.

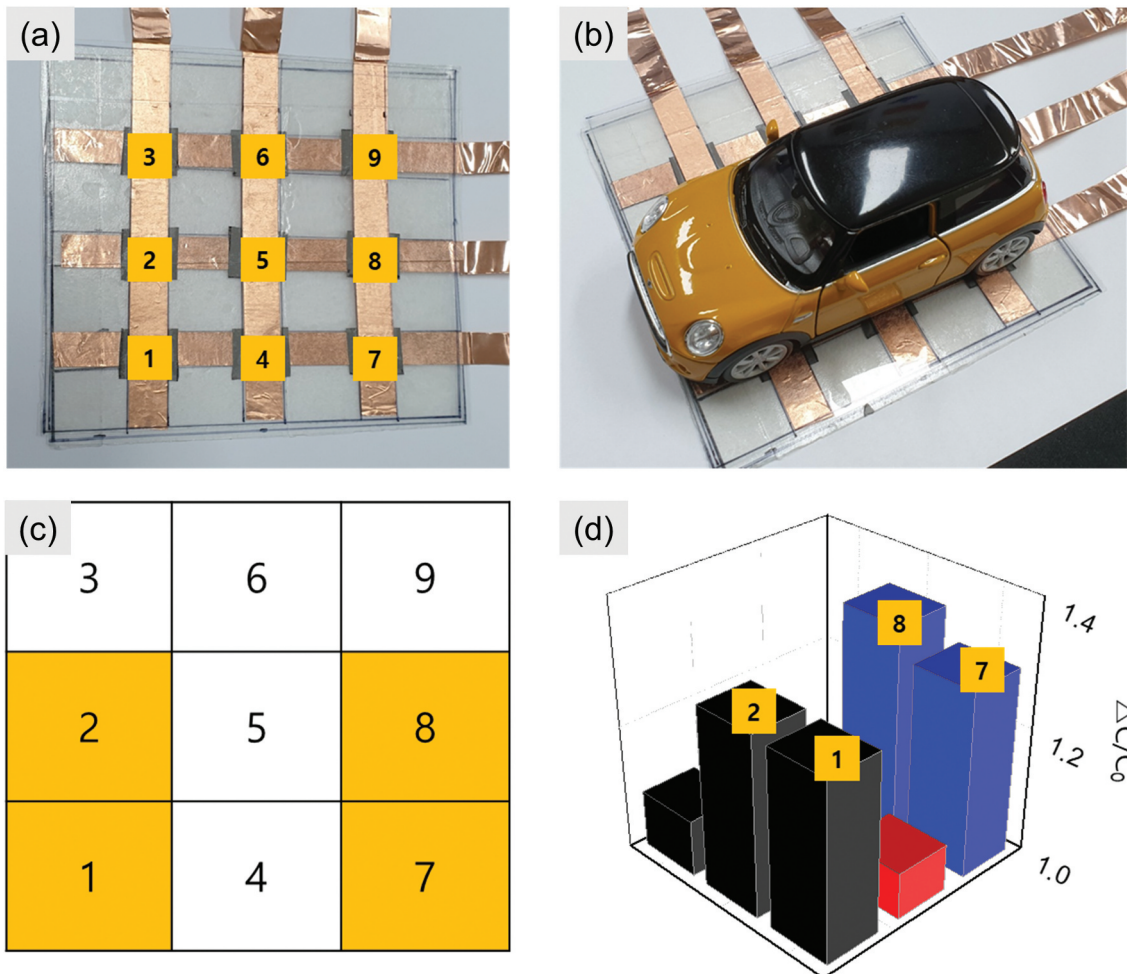


Figure 9. Demonstration of capacitive pressure sensing at the selective area using the 3 x 3 sensor array. Snapshots of (a) the 3 x 3 sensor array. (b) selective contact using a model car, (c) selective contact point, and (d) C/C_0 response of the selective contact area.

showed relatively high C/C_0 response compared to the uncontacted area (Figure 9(d)). These results suggest that the PVDF-GNP composite-based pressure sensor device can be effectively employed in practical environments, irrespective of the movement patterns of the monitored subject.

4. Conclusions

In this study, a novel thin and lightweight composite film comprising PVDF and GNP has been successfully fabricated for the dielectric layer of the capacitive pressure sensor capable of withstanding medium to high pressure ranges. The incorporation of GNP with an average lateral size of $2.55 \pm 0.70 \mu\text{m}$ and an average thickness of $33.74 \pm 10.13 \text{ nm}$ as a filler material notably enhanced the performance of the capacitive pressure sensor, achieving a maximum sensitivity of 4.18 MPa^{-1} within the pressure range of 0.1–1.6 MPa, alongside moderate cycle stability over 1000 cycles. The sensitivity and stability of the pressure sensor surpassed previous reports in the high pressure range (Figure S10). The resulting pressure sensor exhibited a rapid and consistent response time of just a few hundred milliseconds. Moreover, this versatile composite film holds tremendous potential for application in multiple pixel devices, offering practicality in diverse fields such as gait analysis, artificial joints, industrial equipment, prostheses, and custom ergonomic devices. This work represents a significant leap forward, unveiling new prospects for the advancement of capacitive pressure sensors.

Disclosure statement

No potential conflict of interest was reported by the author(s).

Funding

This research was supported by the Clean Production Technology Program of the Korea Evaluation Institute of Industrial Technology (KIET)-granted financial resources from the Ministry of Trade, Industry and Energy, Korea [no. 20000458] and by Korea Institute for Advancement of Technology (KIAT) grant funded by the Korea Government ((MOTIE) [P0008425], The Competency Development Program for Industry Specialist).

Credit author statement

H.K. contributed to methodology, conceptualization, investigation, formal analysis, data curation, visualization, and writing—original draft; M.L. contributed to software, resources, and formal analysis; B.J. contributed to methodology, resources, investigation, and validation; S.-W.P. contributed to resources, investigation, formal analysis; K.Ko contributed to resources, investigation, and formal analysis; J.Y.P. contributed to formal analysis, visualization, and validation; H.S. contributed to

writing—review and editing, and visualization; H.-B.C. contributed to supervision, writing—review and editing; and Y.-H.C. contributed to supervision, conceptualization, project administration, and funding acquisition.

Data availability statement

The authors of this study declare that the data presented in this research, which support the findings, are readily accessible within the paper and its associated supplementary information files. In the event that the raw data files are required in a different format, they can be acquired from the corresponding author upon reasonable request.

References

- [1] Li RQ, Zhou Q, Bi Y, et al. Research progress of flexible capacitive pressure sensor for sensitivity enhancement approaches. *Sens Actuator A*. 2021;321:112425. doi: 10.1016/j.sna.2020.112425
- [2] Mishra RB, El-Atab N, Hussain AM, et al. Recent progress on flexible capacitive pressure sensors: from design and materials to applications. *Adv Mater Technol*. 2021;6(4):2001023. doi: 10.1002/admt.202001023
- [3] Wang HZ, Li Z, Liu ZY, et al. Flexible capacitive pressure sensors for wearable electronics. *J Mater Chem C*. 2022;10:1594–1605. doi: 10.1039/D1TC05304C
- [4] Lei KF, Lee KF, Lee MY. A flexible PDMS capacitive tactile sensor with adjustable measurement range for plantar pressure measurement. *Microsyst Technol*. 2014;20:1351–1358. doi: 10.1007/s00542-013-1918-5
- [5] Masihi S, Panahi M, Maddipatla D, et al. Highly sensitive porous PDMS-Based capacitive pressure sensors fabricated on fabric platform for wearable applications. *ACS Sens*. 2021;6:938–949. doi: 10.1021/acssensors.0c02122
- [6] Li W, Jin X, Zheng YD, et al. A porous and air gap elastomeric dielectric layer for wearable capacitive pressure sensor with high sensitivity and a wide detection range. *J Mater Chem C*. 2020;8:11468–11476. doi: 10.1039/D0TC00443J
- [7] Kumar S, Bijender, Yadav S, et al. Flexible microhyperboloids facets giant sensitive ultra-low pressure sensor. *Sens Actuator A*. 2021;328:112767. doi: 10.1016/j.sna.2021.112767
- [8] Hwang J, Kim Y, Yang H, et al. Fabrication of hierarchically porous structured PDMS composites and their application as a flexible capacitive pressure sensor. *Compos B Eng*. 2021;211:108607. doi: 10.1016/j.compositesb.2021.108607
- [9] Chen SJ, Zhuo BG, Guo XJ. Large area one-step facile processing of microstructured elastomeric dielectric film for high sensitivity and durable sensing over wide pressure range. *ACS Appl Mater Inter*. 2016;8:20364–20370. doi: 10.1021/acsami.6b05177
- [10] Hosseini ES, Chakraborty M, Roe J, et al. Porous elastomer based wide range flexible pressure sensor for autonomous underwater vehicles. *IEEE Sens J*. 2022;22:9914–9921. doi: 10.1109/JSEN.2022.3165560
- [11] Ke K, McMaster M, Christopherson W, et al. Highly sensitive capacitive pressure sensors based on elastomer composites with carbon filler hybrids. *Compos*

- Part A. 2019;126:105614. doi: [10.1016/j.compositesa.2019.105614](https://doi.org/10.1016/j.compositesa.2019.105614)
- [12] Shi YG, Lu XZ, Zhao JH, et al. Flexible capacitive pressure sensor based on microstructured composite dielectric layer for broad linear range pressure sensing applications. *Micromachines Basel*. 2022;13:223. doi: [10.3390/mi13020223](https://doi.org/10.3390/mi13020223)
- [13] Sharma S, Chhetry A, Sharifuzzaman M, et al. Wearable capacitive pressure sensor based on MXene composite nanofibrous scaffolds for reliable human physiological signal acquisition. *ACS Appl Mater Inter*. 2020;12(19):22212–22224. doi: [10.1021/acsami.0c05819](https://doi.org/10.1021/acsami.0c05819)
- [14] Hu WL, Niu XF, Zhao R, et al. Elastomeric transparent capacitive sensors based on an interpenetrating composite of silver nanowires and polyurethane. *Appl Phys Lett*. 2013;102:083303. doi: [10.1063/1.4794143](https://doi.org/10.1063/1.4794143)
- [15] Yao SS, Zhu Y. Wearable multifunctional sensors using printed stretchable conductors made of silver nanowires. *Nanoscale*. 2014;6:2345–2352. doi: [10.1039/c3nr05496a](https://doi.org/10.1039/c3nr05496a)
- [16] Kurup LA, Cole CM, Arthur JN, et al. Graphene porous foams for capacitive pressure sensing. *ACS Appl Nano Mater*. 2022;5:2973–2983. doi: [10.1021/acsnm.2c00247](https://doi.org/10.1021/acsnm.2c00247)
- [17] Kurup LA, Arthur JN, Yambem SD. Highly sensitive capacitive low-pressure graphene porous foam sensors. *ACS Appl Electron Mater*. 2022;4:3962–3972. doi: [10.1021/acsaelm.2c00616](https://doi.org/10.1021/acsaelm.2c00616)
- [18] Geim AK, Grigorieva IV. Van der Waals heterostructures. *Nature*. 2013;499:419–425. doi: [10.1038/nature12385](https://doi.org/10.1038/nature12385)
- [19] Gobre VV, Tkatchenko A. Scaling laws for van der Waals interactions in nanostructured materials. *Nat Commun*. 2013;4:2341. doi: [10.1038/ncomms3341](https://doi.org/10.1038/ncomms3341)
- [20] Yin HY, Liu HB, Wang W, et al. CO₂-induced reversible dispersion of graphene by a melamine derivative. *Langmuir*. 2015;31:12260–12267. doi: [10.1021/acs.langmuir.5b02831](https://doi.org/10.1021/acs.langmuir.5b02831)
- [21] Shang CY, Zhang FM, Xiong YF, et al. Spark plasma forging and network size effect on strength-ductility trade-off in graphene reinforced Ti6Al4V matrix nanocomposites. *Mater Sci Eng*. 2023;862:144480. doi: [10.1016/j.msea.2022.144480](https://doi.org/10.1016/j.msea.2022.144480)
- [22] Zhou KG, Mao NN, Wang HX, et al. A mixed-solvent strategy for efficient exfoliation of inorganic graphene analogues. *Angew Chem Int Edit*. 2011;50:10839–10842. doi: [10.1002/anie.201105364](https://doi.org/10.1002/anie.201105364)
- [23] Mertens M, Van Goethem C, Thijs M, et al. Crosslinked PVDF-membranes for solvent resistant nanofiltration. *J Membrane Sci*. 2018;566:223–230. doi: [10.1016/j.memsci.2018.08.051](https://doi.org/10.1016/j.memsci.2018.08.051)
- [24] Marshall JE, Zhenova A, Roberts S, et al. On the solubility and stability of polyvinylidene fluoride. *Polym Basel*. 2021;13(9):1354. doi: [10.3390/polym13091354](https://doi.org/10.3390/polym13091354)
- [25] Hernandez Y, Lotya M, Rickard D, et al. Measurement of multicomponent solubility parameters for graphene facilitates solvent discovery. *Langmuir*. 2010;26(5):3208–3213. doi: [10.1021/la903188a](https://doi.org/10.1021/la903188a)
- [26] Su Z, Sun XC, Liu XZ, et al. A strategy to prepare high-quality monocrystalline graphene: inducing graphene growth with seeding chemical vapor deposition and its mechanism. *ACS Appl Mater Inter*. 2020;12:1306–1314. doi: [10.1021/acsami.9b16549](https://doi.org/10.1021/acsami.9b16549)
- [27] Lu Y, Liu N, Liu YB, et al. Functionalized graphene grids with various charges for single-particle cryo-EM. *Nat Commun*. 2022;13(1):6718. doi: [10.1038/s41467-022-34579-w](https://doi.org/10.1038/s41467-022-34579-w)
- [28] Dalal MH, Sayyar S, Lee CY, et al. A conductive polymer composite derived from polyurethane and cathodically exfoliated graphene. *Mater Today Chem*. 2023;27:101313. doi: [10.1016/j.mtchem.2022.101313](https://doi.org/10.1016/j.mtchem.2022.101313)
- [29] Ryu SH, Kim S, Kim H, et al. Highly conductive polymer composites incorporated with electrochemically exfoliated graphene fillers. *RSC Adv*. 2015;5(46):36456–36460. doi: [10.1039/C5RA04202J](https://doi.org/10.1039/C5RA04202J)
- [30] Meguid SA, Xia X, Elaskalany M. Unravelling the sensory capability of MWCNT-reinforced nanocomposites: experimental and numerical investigations. *Carbon*. 2023;204:147–161. doi: [10.1016/j.carbon.2022.12.037](https://doi.org/10.1016/j.carbon.2022.12.037)
- [31] Ismail N, Essalhi M, Rahmati M, et al. Experimental and theoretical studies on the formation of pure β -phase polymorphs during fabrication of polyvinylidene fluoride membranes by cyclic carbonate solvents. *Green Chem*. 2021;23(5):2130–2147. doi: [10.1039/D1GC00122A](https://doi.org/10.1039/D1GC00122A)
- [32] Chatterjee A, Das A, Saha K, et al. Nanofiller-induced enhancement of PVDF electroactivity for improved sensing performance. *Adv Sens Res*. 2023;2(6):2200080. doi: [10.1002/adsr.202200080](https://doi.org/10.1002/adsr.202200080)
- [33] Chang ES, Ameli A, Alian AR, et al. Percolation mechanism and effective conductivity of mechanically deformed 3-dimensional composite networks: computational modeling and experimental verification. *Composites Part B*. 2021;207:108552. doi: [10.1016/j.compositesb.2020.108552](https://doi.org/10.1016/j.compositesb.2020.108552)
- [34] Haghayegh M, Cao R, Zabihi F, et al. Recent advances in stretchable, wearable and bio-compatible triboelectric nanogenerators. *J Mater Chem C*. 2022;10(32):11439–11471. doi: [10.1039/D2TC01931K](https://doi.org/10.1039/D2TC01931K)
- [35] Moghadam BH, Hasanzadeh M, Simchi A. Self-powered wearable piezoelectric sensors based on polymer nanofiber–metal–organic framework nanoparticle composites for arterial pulse monitoring. *ACS Appl Nano Mater*. 2020;3:8742–8752. doi: [10.1021/acsnm.0c01551](https://doi.org/10.1021/acsnm.0c01551)
- [36] Kabir H, Kamali Dehghan H, Mashayekhan S, et al. Hybrid fibrous (PVDF-BaTiO₃)/PA-11 piezoelectric patch as an energy harvester for pacemakers. *J Ind Text*. 2022;51(3_suppl):4698S–4719S. doi: [10.1177/15280837211057575](https://doi.org/10.1177/15280837211057575)
- [37] Jin T, Pan Y, Jeon GJ, et al. Ultrathin nanofibrous membranes containing insulating microbeads for highly sensitive flexible pressure sensors. *ACS Appl Mater Interfaces*. 2020;12:13348–13359. doi: [10.1021/acsami.0c00448](https://doi.org/10.1021/acsami.0c00448)